Dielectric, mechanical and rheological studies of phase separation and cure of a thermoplastic modified epoxy resin: incorporation of reactively terminated polysulfones

Alexander J. MacKinnon*, Stephen D. Jenkins†, Patrick T. McGrail† and Richard A. Pethrick

Department of Pure and Applied Chemistry, University of Strathclyde, Thomas Graham Building, 295 Cathedral Street, Glasgow G1 1XL, UK

†ICI plc, Wilton Materials Research Centre, Wilton, Middlesbrough, Cleveland TS6 8JE, UK

(Received 24 April 1992; revised 21 December 1992)

Application of dielectric, mechanical and rheological measurements to the characterization of cure and phase separation in a thermoplastic modified epoxy resin is reported. These data indicate that the dielectric technique is not only useful for monitoring changes in network dynamics during the process of cure, but can also provide valuable information on the phase separation of the occluded phase. The paper discusses the modelling of the dielectric data, and considers the importance of understanding the relationship between morphology and mechanical properties.

(Keywords: phase separation; curing; epoxy resin)

INTRODUCTION

Dielectric measurements on polymers have undergone a renaissance in the last few years with the advent of computer assisted data collection[1–3]. Frequency dependent electromagnetic sensing (FDEMS) has been proposed as a convenient, automated and highly sensitive technique for the study of reactive systems. The FDEMS method can be used for quality control of resins, characterization of the variation of cure properties with resin formulation, simulation of the effects of changing processing variables (temperature and pressure on the cure process), and continuous monitoring of cure *in situ* in the manufacturing tool[4]. A correlation has been proposed between variations observed in the dielectric properties of the resin during the cure process and changes in the rheological properties. In a recent paper, the use of the dielectric method for the characterization of morphology was demonstrated using a system of dispersed conducting occlusions; cylinders of ionically doped poly(ethylene oxide) in polycarbonate[4]. The aim of this study was to investigate structure–property relationships for a thermoplastic modified epoxy resin, as well as the application of the dielectric method for the characterization of cure and the study of morphology.

Epoxy resins are one of the most important classes of thermosetting polymers, and are widely used as structural adhesives and in composite manufacture[5–7]. Unfortunately, these highly crosslinked networks are inherently brittle, and consequently have limited utility in applications requiring high impact strength, or resistance to damage induced by thermal cycling[8]. In recent years, incorporation of elastomeric modifiers has been proposed as a method of enhancing the fracture strength of these brittle materials[8]. Linear, high molecular weight thermoplastics are also inherently tough however, and can be expected to reduce the brittleness of a thermoset without affecting its other properties significantly. Bucknall and Partridge[9,10] have used polyethersulfones from ICI in epoxy resins to generate high temperature thermoplastic modified thermosets. This approach allows toughening to be achieved without significantly lowering the glass transition temperature (T_g). The addition of rubber tougheners usually leads to a lowering of the T_g, and consequent loss of high temperature mechanical properties. Subsequently, different thermoplastics have been studied in epoxy resins by Bucknall and Gilbert[11], McGrath and co-workers[12,13] and Sefton and co-workers[14]. Thermoplastics have also been studied in other types of thermoset networks[15–18]. The thermoplastics and thermosets used in this study were chosen to be thermodynamically compatible[19,20]; however, during the curing process it is now recognized that the increasing molecular weight of the thermoset component initiates phase separation. This generates a heterogeneous cured material, which may exhibit particulate, co-continuous or phase-inverted morphology[14].

Increases in the viscosity associated with the curing process may be measured using conventional oscillatory

*To whom correspondence should be addressed

0032-3861/93/153252-12

cone-and-plate rheometers; however, it is rather difficult to use these instruments to monitor the change in viscosity over the whole process of cure[21,22]. An alternative approach to this problem has recently been published[23], which allows the rheology to be examined throughout the entire period of cure. In this paper, rheological and dielectric measurements are reported during cure, and thermal, dielectric and mechanical properties are also presented for completely cured thermoplastic modified epoxy resins.

EXPERIMENTAL

Materials

The modified thermoset system was based on the cure of triglycidyl aminophenol (Ciba Geigy, MY0510) with 4,4′-diaminodiphenylsulfone (4,4′-DDS, Ciba Geigy HT976), and the thermoplastic was either an amine-terminated [RT-PS(A)] ($M_n = 11\,000$, $R_v = 0.20$–0.24) or an epoxidized [RT-PS(B)] ($M_n = 13\,000$, $R_v = 0.24$–0.28) polysulfone synthesized for this project. Comparison of the RT-PS/epoxy resin blends is also made with similar blends incorporating ICI PES 5003P as the thermoplastic component. 5003P is a hydroxy terminated polysulfone ($M_n = 24\,000$, $R_v = 0.50$–0.52) and produces similar morphologies to the systems studied in this work, with the exception that the phase sizes are considerably larger. The epoxy resin and hardener were used as supplied in the ratio of 2.1:1 (wt/wt), whilst the thermoplastic was dried before use. Cure samples were made by dissolving the thermoplastic in a 95:5 (v/v%) mixture of methylene chloride and methanol. The curing agent was added to the solution of the epoxy/thermoplastic mixture before the solvent was boiled off, leaving a homogeneous solution. This blend was poured into an open mould (15 cm × 10 cm), which had been preheated to 413 K, and then degassed for 30 min under vacuum to remove residual solvent and trapped air. For dielectric and rheological measurements, the mould was removed from the oven and cooled rapidly to quench the curing reaction and stored at 253 K until needed. The samples for mechanical and electron microscopic examination, however, were cured at 453 K for a further 120 min, and then allowed to cool slowly to room temperature. A range of samples with varying thermoplastic content was made in each case.

Real time dielectric measurements

Dielectric measurements were performed using a Solatron 1250 frequency response analyser; the method used for interfacing the instrument to the sample and the procedures used for data analysis have been described previously[1]. Data were collected between 10^{-1} Hz and 6.3×10^4 Hz in a period of <3 min. The system was programmed to store successive sets of data, and allowed real time examination of the cure process for all the mixtures. A cell consisting of two pre-etched copper electrodes mounted on an epoxy glass fibre base was used for studies of the liquid material. This design generated a three-electrode system with an active electrode area of 1 cm^2, and was placed in an Oxford Instruments cryostat (DN1704). The space between the electrodes was maintained constant with a copper spacer, and the outer guard rings of both electrodes and spacer were soldered together to form a seal around three edges. The resin to be studied was injected as a liquid into the cell, capillary action ensuring the cell was completely filled. The electrodes were in good thermal contact with a copper block, which was used to maintain the temperature of the sample at that required for the isothermal cure studies.

Rheological measurements

A curometer, designed at Strathclyde[23], was used to monitor changes in the viscosity with time at 2 Hz, and also the curing exotherm. The instrument was calibrated using Santovac-5, which was chosen because it exhibited a very high temperature–viscosity coefficient, and formed a stable, supercooled liquid state, which has been studied extensively[24,25].

D.s.c. measurements

D.s.c. measurements were conducted using a Du Pont model 9900 calorimeter. In all cases a sample of ~ 10 mg was used at a heating rate of 10°C min^{-1}, over a temperature range of -50 to 300°C. In these experiments, the sample was cured during the first temperature scan, allowing evaluation of the heat of reaction. The sample was then cooled slowly to room temperature, and a second scan used to determine the final T_g. A further series of experiments was then carried out on samples from the plaques prepared for mechanical testing, in order to estimate the degree of cure at 180°C, and also to determine their final T_gs.

Mechanical testing

Mechanical properties were assessed at 23°C on moulded plaques, and the following parameters considered: flexural modulus was determined by a three-point bend test at 5 mm min^{-1}, using a sample size of 50 mm × 10 mm × 3 mm; yield strength, σ_y, was obtained in compression using a sample size of 10 mm × 10 mm × 3 mm; mode I stress intensity factor, K_{Ic}, was measured at 1 mm min^{-1} using a sample size of 70 mm × 10 mm × 3 mm with a single edge notched on the 10 mm face; and mode I strain energy release rate, G_{Ic}, was also measured under these conditions. Finally, the ductility factor, $(K_{Ic}/\sigma_y)^2$, was derived from these data[8]. The test methods used have been reported fully elsewhere[26].

THEORY FOR THE ANALYSIS OF DIELECTRIC BEHAVIOUR OF HETEROGENEOUS SYSTEMS

Previous studies[14] of cured epoxy/thermoplastic blends have indicated that they possess a phase separated structure, the morphology depending critically on the level of thermoplastic in the matrix material. Phase separation leading to the generation of occluded domains which have a higher conductivity than the surrounding matrix, can produce materials which exhibit distinct dielectric behaviour[27–36]. Application of an electric field leads to migration of charges within the occluded phase, the diffusion distance depending on the orientation of the domain, and the rate on the conductivity. The polarization which results can be several orders of magnitude larger than that typically observed for dipolar relaxation processes. Studies on model systems[34] and phase-separated polymers, such as styrene–butadiene–

styrene[32], have shown a unique relationship between the morphological structure of these materials and their dielectric response.

A polar organic material may exhibit frequency-dependent dielectric properties described in terms of the complex permittivity[30]:

$$\varepsilon^*(\omega)=\varepsilon'(\omega)-i\varepsilon''(\omega) \quad (1)$$

where $\varepsilon'(\omega)$ and $\varepsilon''(\omega)$ are the real and imaginary parts of the dielectric permittivity, and $i=\sqrt{-1}$. A simple dipolar medium exhibits a frequency dependence which has the form:

$$\frac{\varepsilon'(\omega)-\varepsilon'_\infty}{\varepsilon'_0-\varepsilon'_\infty}=\frac{1}{1+\omega^2\tau^2} \quad (2)$$

and

$$\frac{\varepsilon''(\omega)}{\varepsilon'_0-\varepsilon'_\infty}=\frac{\omega\tau}{1+\omega^2\tau^2} \quad (3)$$

Here ε'_0 and ε'_∞ are, respectively, the low and high frequency limiting values of the dielectric permittivity for a process with characteristic relaxation time τ. Equations (2) and (3) are interrelated via a Laplace transform according to Kramers Kronig[30]. Analysis to produce data on the dipolar relaxation process has been presented elsewhere[35,36].

DIELECTRIC PROPERTIES OF HETEROPHASE SYSTEMS

The theory of heterogeneous dielectrics has been reviewed by van Beek[28]. In the case of spheres or ellipsoids of conductivity σ_2 and permittivity ε'_2 dispersed in a homogeneous matrix (σ_1, ε'_1), the dielectric properties are described by the Maxwell–Wagner–Sillars (MWS) model. The characteristic relaxation time, τ_{MWS}, and low frequency limiting value of the permittivity, ε_s, are described as follows:

$$\tau_{MWS}=\left[\frac{\varepsilon'_1+A_a(1-v_2)(\varepsilon'_2-\varepsilon'_1)}{\sigma_1+A_a(1-v_2)(\sigma_2-\sigma_1)}\right]\varepsilon_0 \quad (4)$$

$$\varepsilon_s=\varepsilon'_1\frac{\sigma_1[A_a(1-v_2)+v_2](\sigma_2-\sigma_1)}{\sigma_1+A_a(1-v_2)(\sigma_2-\sigma_1)}+v_2\sigma_1 \times\frac{\sigma_1+A_a(\sigma_2-\sigma_1)(\varepsilon'_2-\varepsilon'_1)-[\varepsilon'_1+A_a(\varepsilon'_2-\varepsilon'_1)](\sigma_2-\sigma_1)}{[\sigma_1+A_a(1-v_2)(\sigma_2-\sigma_1)]^2} \quad (5)$$

and ε_∞ is the limiting value of the high frequency permittivity:

$$\varepsilon_\infty=\frac{\varepsilon'_1+[A_a(1-v_2)+v_2](\varepsilon'_2-\varepsilon'_1)}{\varepsilon'_1+A_a(1-v_2)(\varepsilon'_2-\varepsilon'_1)}\varepsilon'_1 \quad (6)$$

where A_a is the depolarization factor along the applied field axis, v_2 is the volume fraction of the occluded phase, and the ε'_1 value is the low frequency limiting permittivity for phase 1. For the special case of spheres or ellipsoids of conductivity σ_2 and permittivity ε'_2 dispersed in a homogeneous medium (σ_1, ε'_1), the depolarizing factor along the a-axis of the ellipsoid, A_a, has the form:

$$A_a=\frac{-1}{(a/b)^2-1}+\frac{a/b}{[(a/b)^2-1]^{1.5}}\ln\{(a/b)+[(a/b)^2-1]^{1/2}\}$$

for the case of prolate spheroids ($a>b$), where a is the length along the major axis and b along the minor axis, and:

$$A_a=\frac{1}{1-(a/b)^2}-\frac{(a/b)}{[1-(a/b)^2]^{1.5}}\arccos(a/b)$$

for the case of oblate spheroids ($a<b$). For the case of spheres where $a=b$, then $A_a=1/3$.

In practice, for lossy material dispersed in a polymeric insulator, i.e. $\sigma_2\gg\sigma_1$ and $v_2\ll v_1$, the following relationships apply:

$$\tau_{MWS}\simeq\left[\frac{\varepsilon'_1+A_a(\varepsilon'_2-\varepsilon'_1)}{A_a\sigma_2}\right]\varepsilon_0 \quad (4)$$

$$\varepsilon_\infty\simeq\varepsilon'_1\left[1+v_2\frac{\varepsilon'_2-\varepsilon'_1}{\varepsilon'_1+A_a(\varepsilon'_2-\varepsilon'_1)}\right] \quad (6)$$

The above equations provide the basis for analysis of the dielectric properties of heterogeneous materials, and will be used to investigate the form of the dielectric response of the fully cured MY0510/4,4′-DDS/RT-PS(A) and MY0510/4,4′-DDS/RT-PS(B) samples. The validity of the above equations has been recently tested, by the description of the dielectric relaxation processes observed in model systems, and they have been shown to provide an accurate fit to the dielectric data obtained[34]. This study indicated that for the model system concerned, once the appropriate parameters had been set, the temperature dependence could be accurately predicted from the variation of the conductivity of the occluded phase.

RESULTS AND DISCUSSION

Previous studies of polysulfone modified epoxy resins have established that the thermoplastic is phase separated in the cured material[14,37,38]. It is important to determine the point during cure at which phase separation occurs, and to describe as accurately as possible the nature and dispersion in size of the domains present. The effectiveness of thermoplastics as toughening agents in thermoset applications depends upon a number of factors, particle size being particularly important in controlling the brittle–tough transition temperature[39–42]. Toughening is generally explained through crazing or shear yielding mechanisms, but cavitation in or around an impact modifying particle can also make an important contribution in this respect. The distribution in particle or other domain sizes within the cured matrix is, therefore, of importance in understanding the toughening mechanisms in these materials.

Curometer data

The rheology of mixtures with varying thermoplastic content was examined using the Strathclyde curometer in order to determine their pot-life and gel times. Plots of the real and imaginary responses, and the computed viscosities for cure carried out at 453 K, are presented in *Figures 1a–c*. The addition of thermoplastic to the thermoset matrix inhibits the cure as indicated by the gel time, estimated from the point at which the viscosity reaches a value of 10^4 Pa s (*Table 1*). It was not possible to monitor the rheology of systems containing <20% thermoplastic at 453 K, owing to the highly exothermic nature of the epoxy resin reaction. At higher thermoplastic content it appears, therefore, that the polymer acts as a

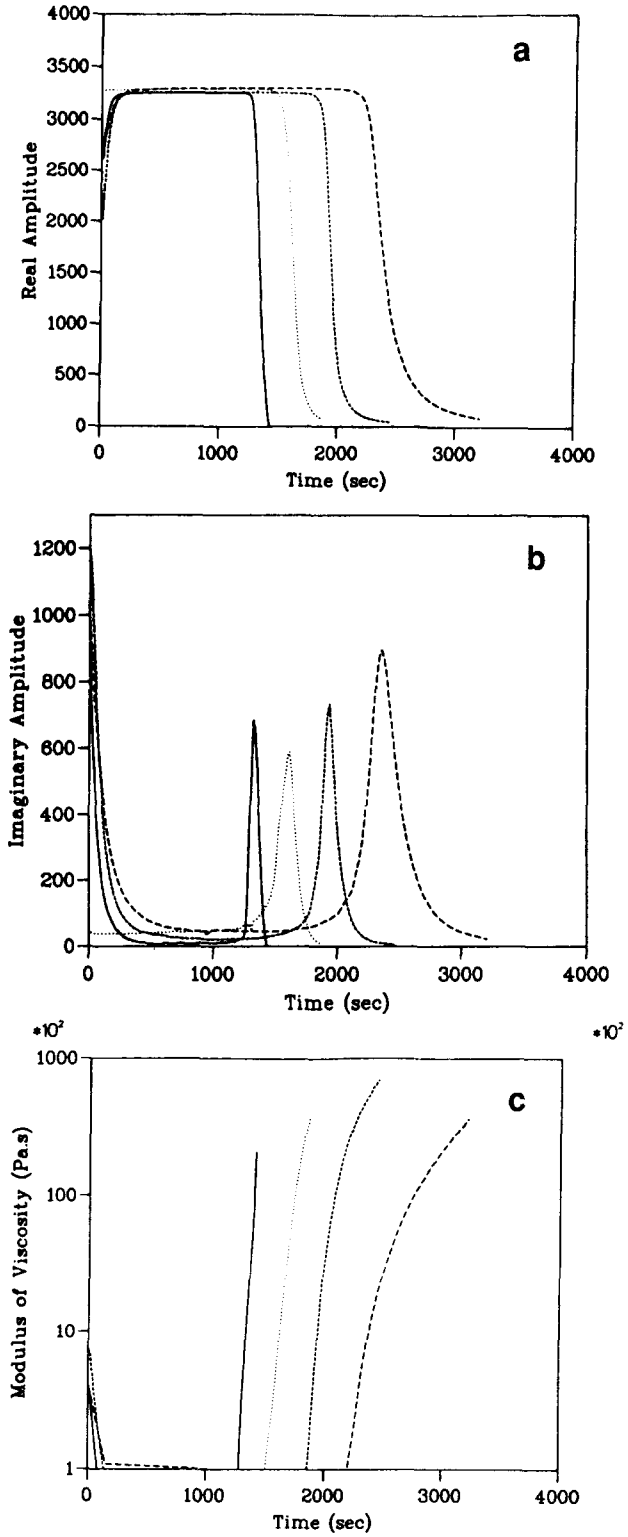

Figure 1 Cure of MY0510/4,4'-DDS/RT-PS(A) monitored by curometer at 180°C. Plots of (a) real amplitude, (b) imaginary amplitude and (c) modulus of viscosity, *versus* time. ——, MY0510/4,4'-DDS/26.7% RT-PS(A); ·····, MY0510/4,4'-DDS/30.0% RT-PS(A); -----, MY0510/4,4'-DDS/34.6% RT-PS(A); – – –, MY0510/4,4'-DDS/39.1% RT-PS(A)

diluent, inhibiting the reaction and reducing the rate at which heat is liberated.

D.s.c. measurements

The initial mixture and completely cured materials were subjected to d.s.c. analysis as described above. Variations of the heat of cure and the T_gs for the various compositions investigated are presented in *Table 2*. The curing exotherm decreased linearly with increasing thermoplastic content, and no significant deviations from simple additivity were observed. In these systems, the T_g of the cured unmodified epoxy resin differs significantly from those of the epoxy/thermoplastic blends (*Table 2*). For both the RT-PS(A) and RT-PS(B) series, there is a progressive decrease in the value of T_g with increasing thermoplastic content up to ~20 wt%. This decrease is consistent with compatibility of the thermoplastic and thermoset to a limited extent, leading to the observation of a diminution of the value of the epoxy T_g. Above 20 wt%, the value of the T_g becomes almost constant indicating no further effect of addition of thermoplastic. Previous electron microscopy studies have indicated that below 20 wt% the morphology conforms to a dispersion of spheres of thermoplastic-rich material in an epoxy-rich matrix. The depression of T_g initially is consistent with the dissolution of the thermoplastic to a limited extent in the epoxy resin, leading to an increase in the free volume and a lowering of T_g. Above ~20 wt% thermoplastic the system undergoes morphological change to co-continuous phases and then phase inversion. In the latter the continuous phase becomes thermoplastic-rich, and the occluded phase epoxy-rich. The apparent concentration independent value of T_g is consistent with the thermoplastic gradually forming a matrix into which is dissolved a small amount of the epoxy resin. A single T_g was observed in all blends due to the close proximity of the T_g values for the individual components and there is, therefore, little actual variation of T_g with the amount of thermoplastic added.

Electron micrographs for related systems have been reported previously[14,36–38] and indicate changes in the phase structure with composition. In the case of the present systems between 0 wt% and 2.5 wt% thermoplastic, a homogeneous solution is observed. Concentrations in the range 5–20 wt% produce a particulate phase, which changes into a co-continuous phase at 25–30 wt%. Above 30 wt% phase inversion occurs, the continuous phase now being thermoplastic-rich. The changes which occur are illustrated schematically in *Figure 2a*, and confirmed from micrographs obtained from these materials (*Figures 2b–d*). The size distributions of the occluded phases are illustrated in *Table 3*. It would appear from *Figures 2b–d* that the morphological scale size is strongly dependent on thermoplastic molecular weight and/or end group functionality. The RT-PS(B) series shows substantially finer morphologies than those with RT-PS(A), although the type of morphology/phase separation remains unchanged.

Mechanical properties of epoxy/thermoplastic blends

The mechanical properties of the RT-PS(A) blends are shown in *Figures 3a–e* in conjunction with the 5003P blends for comparison[37]. No data are available for pure RT-PS(A) as this material is too brittle to produce test specimens.

The flexural moduli for the set of RT-PS(A) blends shows little correlation with the level of thermoplastic present, and there would appear to be little difference between these data and those for the set of 5003P blends. The yield strengths of the RT-PS(A) show a distinct decrease in magnitude with increasing thermoplastic content, before levelling off at ~25 wt%. This point would appear to be consistent with the generation of the

Table 1 Cure data of MY0510/4,4'-DDS/RT-PS(A) and MY0510/4,4'-DDS/RT-PS(B) blends at 180°C

MY0510/4,4'-DDS/RT-PS(A) blends						MY0510/4,4'-DDS/RT-PS(B) blends					
RT-PS(A) (wt%)	Vitrification time (min)			Pot life (min)	Gelation time (min)	RT-PS(B) (wt%)	Vitrification time (min)			Pot life (min)	Gelation time (min)
	ε'[a]	ε''[b]	σ' d.c.[c]	η[d]	η[e]		ε'[a]	ε''[b]	σ' d.c.[c]	η[d]	η[e]
0	66.7	67.6	75.0	–[f]	–	0	66.7	67.6	75.0	–	–
5.4	84.6	73.6	83.6	–	–	5.4	48.3	56.7	68.8	–	–
11.0	115.5	140.0	113.6	–	–	11.0	85.6	140.5	125.9	–	–
15.6	153.6	136.7	155.6	–	–	15.6	97.2	130.0	140.0	–	–
20.5	112.7	89.1	71.8	–	–	20.5	100.5	149.1	131.4	–	–
26.7	50.0	51.8	64.5	19.0	23.3	26.7	56.3	100.0	95.8	17.8	20.0
30.0	132.7	101.8	122.7	20.8	28.8	30.0	68.2	117.9	135.0	19.2	23.7
34.6	121.8	103.6	112.7	23.0	34.7	34.6	93.0	145.6	123.0	23.4	27.0
39.1	91.7	78.1	89.7	36.8	46.3	39.1	93.1	150.0	180.0	30.6	35.0

[a]Vitrification point from levelling off of ε' at 10^4 Hz
[b]Vitrification point from levelling off of ε'' at 10^4 Hz
[c]Vitrification point from levelling off of σ' d.c.
[d]Pot life from 5% increase in η
[e]Gel point from $\eta = 10^4$ Pa s
[f]Not applicable

Table 2 D.s.c. of MY0510/4,4'-DDS/RT-PS(A) and MY0510/4,4'-DDS/RT-PS(B) blends

MY0510/4,4'-DDS/RT-PS(A) blends					MY0510/4,4'-DDS/RT-PS(B) blends		
RT-PS(A) (wt%)	ΔH_{cure}[a] (J g^{-1})	T_g[b] (°C)	$\Delta H_{postcure}$[c] (J g^{-1})	T_g[d] (°C)	RT-PS(B) (wt%)	ΔH_{cure} (J g^{-1})	T_g (°C)
0.0	666.7	237.3	35.3	222.1	0.0	666.7	237.3
5.4	700.7	227.1	61.7	212.7	5.4	621.5	217.7
11.0	594.1	217.6	72.5	219.4	11.0	536.2	210.8
15.6	555.1	202.6	52.2	190.9	15.6	438.4	194.3
20.6	506.5	188.0	46.5	196.1	20.6	530.1	181.9
26.7	415.2	207.0	57.3	203.1	26.7	549.4	192.3
30.0	431.8	208.3	112.2	196.6	30.0	476.2	214.1
34.6	386.4	199.9	96.3	201.0	34.6	450.3	193.7
39.1	393.3	191.5			39.1	417.2	194.5

[a]Cure reaction
[b]Rerun of sample from footnote *a* – T_g determination
[c]Post-cure reaction of samples prepared at 180°C for mechanical testing
[d]Rerun of sample from footnote *c* – T_g determination

co-continuous morphology. Comparing the two sets of blends, the RT-PS(A) blends show an appreciable drop in yield strength in comparison to the 5003P blends. The K_{Ic} and G_{Ic} values of the RT-PS(A) series show similar trends to those with 5003P. In both cases there is a distinct increase in toughness at 20 wt% thermoplastic, again consistent with the adoption of a co-continuous morphology. Comparison of the RT-PS(A) and 5003P blends shows that both sets have similar G_{Ic} values up to 20 wt% thermoplastic. Thereafter the 5003P series has the greater toughness. This may well be attributed to the different end groups or increased molecular weight of the 5003P thermoplastic, or the consequent change in the thermoplastic-rich phase size. The effects of increasing the molecular weight of the thermoplastic have been recently discussed[43], and the general trends observed by these workers are in agreement with the current findings. It should however be pointed out that whilst they recognized the effects of molecular weight, they have not discussed the critical importance of the co-continuous and phase-inverted regions upon these mechanical properties.

Dielectric measurements

Measurements were performed on samples curing isothermally at 453 K as a function of thermoplastic content, and three-dimensional plots for various composition were obtained. Plots for 0, 26.7 and 39.1% are shown in *Figures 4a–f* for the MY0510/4,4'-DDS/RT-PS(A) blend. Similar traces were obtained for the MY0510/4,4'-DDS/RT-PS(B) series; however, the residual low frequency increment at high thermoplastic content was significantly smaller possibly due to decrease in morphological scale size. All the traces showed three distinct relaxation features. At low frequency and short times, a large dielectric loss is observed which rapidly decreases as cure proceeds and can be attributed to blocking electrode effects[44–46]. A high level of direct current (d.c.) conductivity, characterized by an approxi-

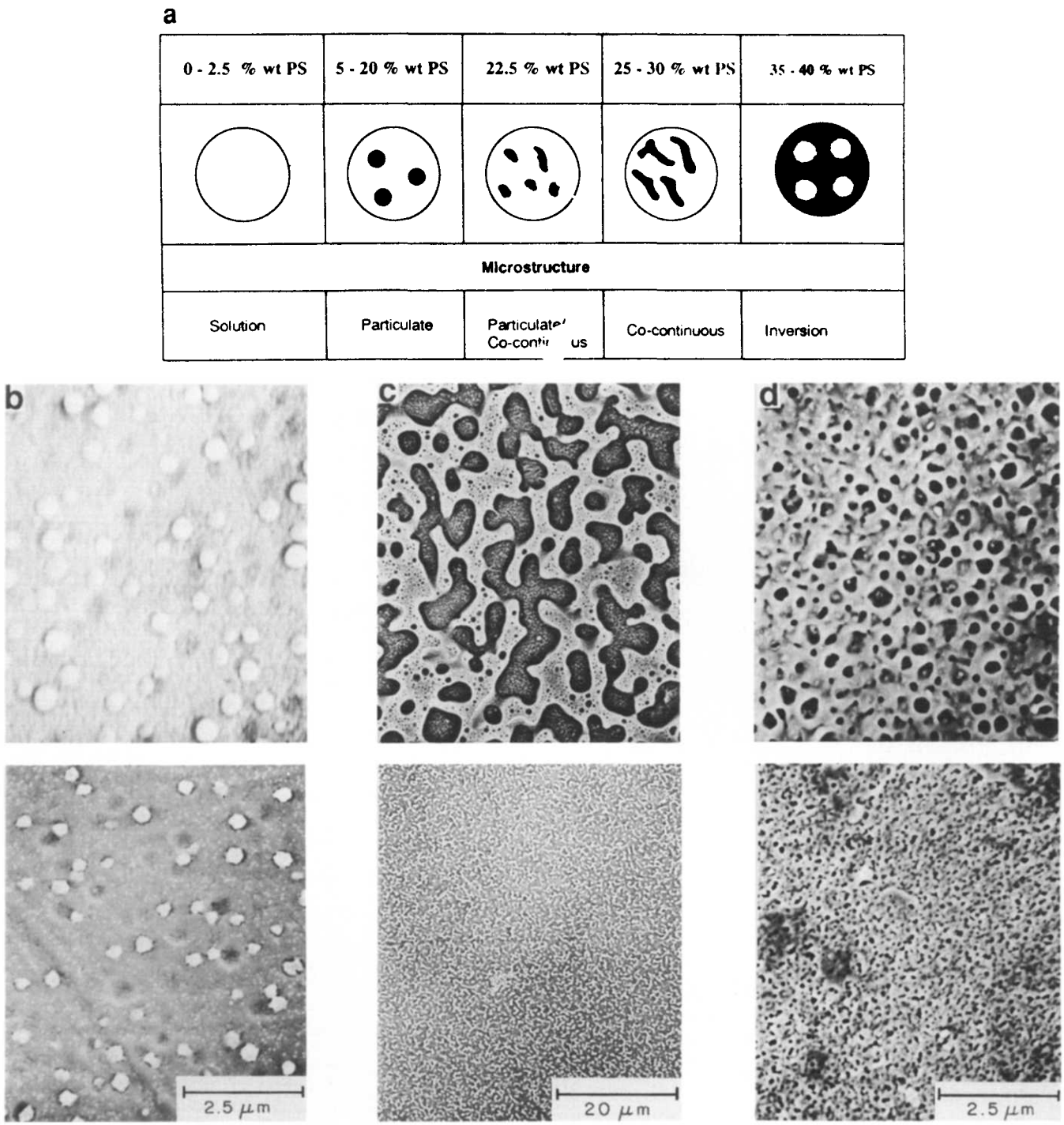

Figure 2 (a) Schematic diagram of the variation of morphological types with composition for MY0510/4,4'-DDS/PS. (b)–(d) Scanning electron micrographs [upper, RT-PS(A); lower, RT-PS(B)] of cured specimens from dielectric studies: (b) 5.4: (c) 26.7; (d) 39.1 wt% thermoplastic

mately -1 slope of $(\delta \log \varepsilon''/\delta \log f)$, is observed initially, and this is reduced during cure. However, in many of the samples, a significant d.c. conductivity is still clearly evident in the fully cured matrix (*Table 4*). These values indicate a reduction in the conductivity with increasing thermoplastic content, the scatter in the data being too large to make any further detailed discussion. The variation in conductivities of the cured epoxy/thermoplastic blends can be attributed to the presence of impurities within the resins and blends. The dipolar relaxation, observed as a peak in the loss at high frequencies, and leading to a step in the dielectric constant (*Table 1*), is associated with vitrification of the matrix.

The curves obtained with low levels of thermoplastic (5.4 wt%), are very similar to those obtained for the pure resin material. Further increase in the concentration of thermoplastic causes the dipolar process to become difficult to resolve, and vitrification to be extended to longer times. The magnitude of the d.c. conductivity is reduced and an additional feature is observed in the

Table 3 Size distributions of the occluded phase in various epoxy/polysulfone blends

System	Size distributions of occluded phase (μm)	
5003P[a]	20.0%: 1.14–1.82	30.0%: 1.08–3.23
RT-PS(A)[b]	20.0%: 0.15–0.60	35.0%: 0.06–1.00

[a]From ref. 37
[b]From ref. 38

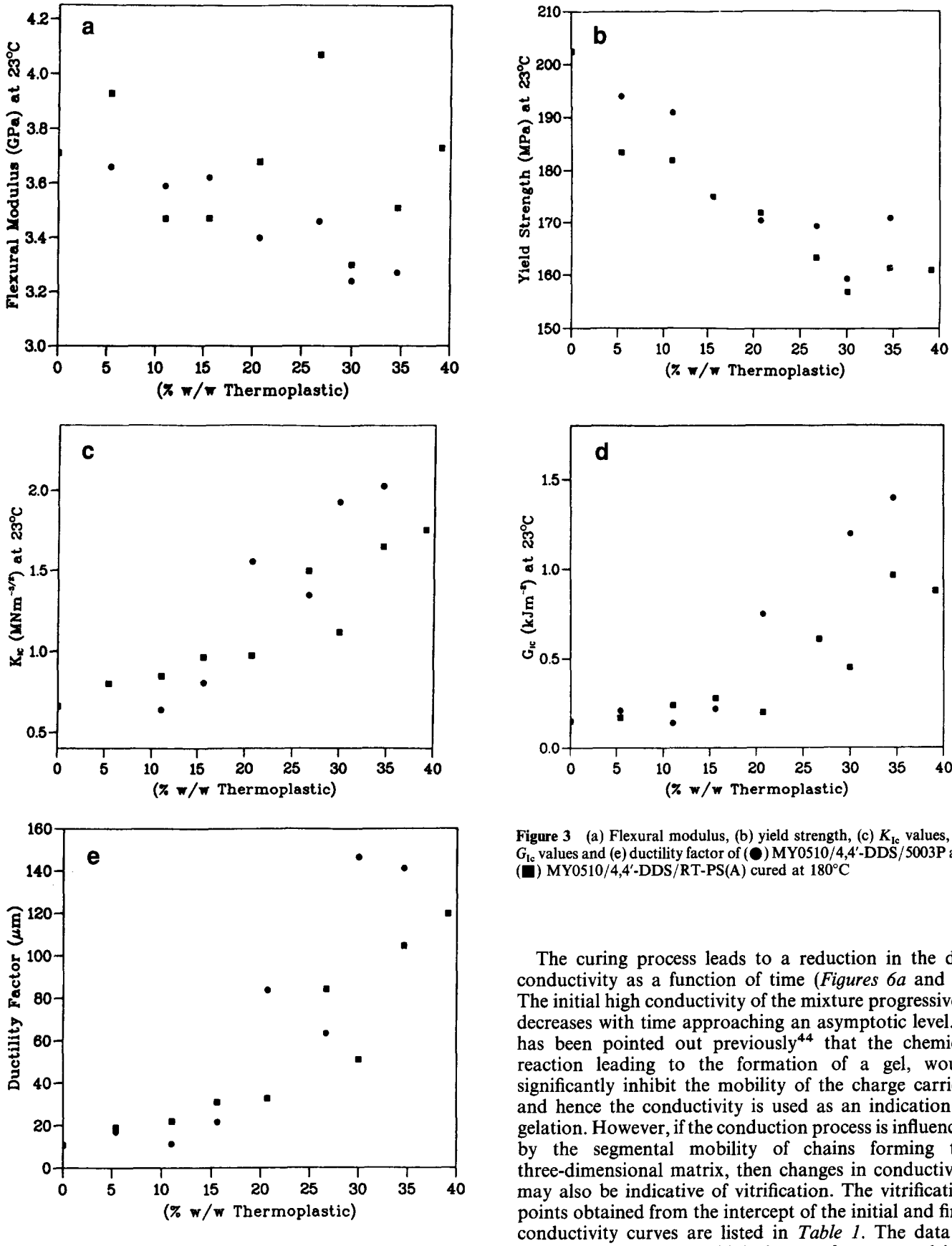

Figure 3 (a) Flexural modulus, (b) yield strength, (c) K_{Ic} values, (d) G_{Ic} values and (e) ductility factor of (●) MY0510/4,4′-DDS/5003P and (■) MY0510/4,4′-DDS/RT-PS(A) cured at 180°C

finally cured material for compositions of >20 wt% thermoplastic. At compositions of 26.7 wt% thermoplastic and above, this feature has now developed into a distinct relaxation process independent of the time of cure. *Figures 5a–h* (experimental data) illustrate more clearly the appearance of this feature.

The curing process leads to a reduction in the d.c. conductivity as a function of time (*Figures 6a* and *b*). The initial high conductivity of the mixture progressively decreases with time approaching an asymptotic level. It has been pointed out previously[44] that the chemical reaction leading to the formation of a gel, would significantly inhibit the mobility of the charge carriers and hence the conductivity is used as an indication of gelation. However, if the conduction process is influenced by the segmental mobility of chains forming the three-dimensional matrix, then changes in conductivity may also be indicative of vitrification. The vitrification points obtained from the intercept of the initial and final conductivity curves are listed in *Table 1*. The data in *Tables 1* and *4* show a high degree of scatter and it is difficult to establish any trend with thermoplastic concentration. Irregularities may be attributed to the following:

1. The vitrification point is obtained from the intercept of the slope of the steadily decreasing ε' or ε'' values, and at the point at which these values reach an

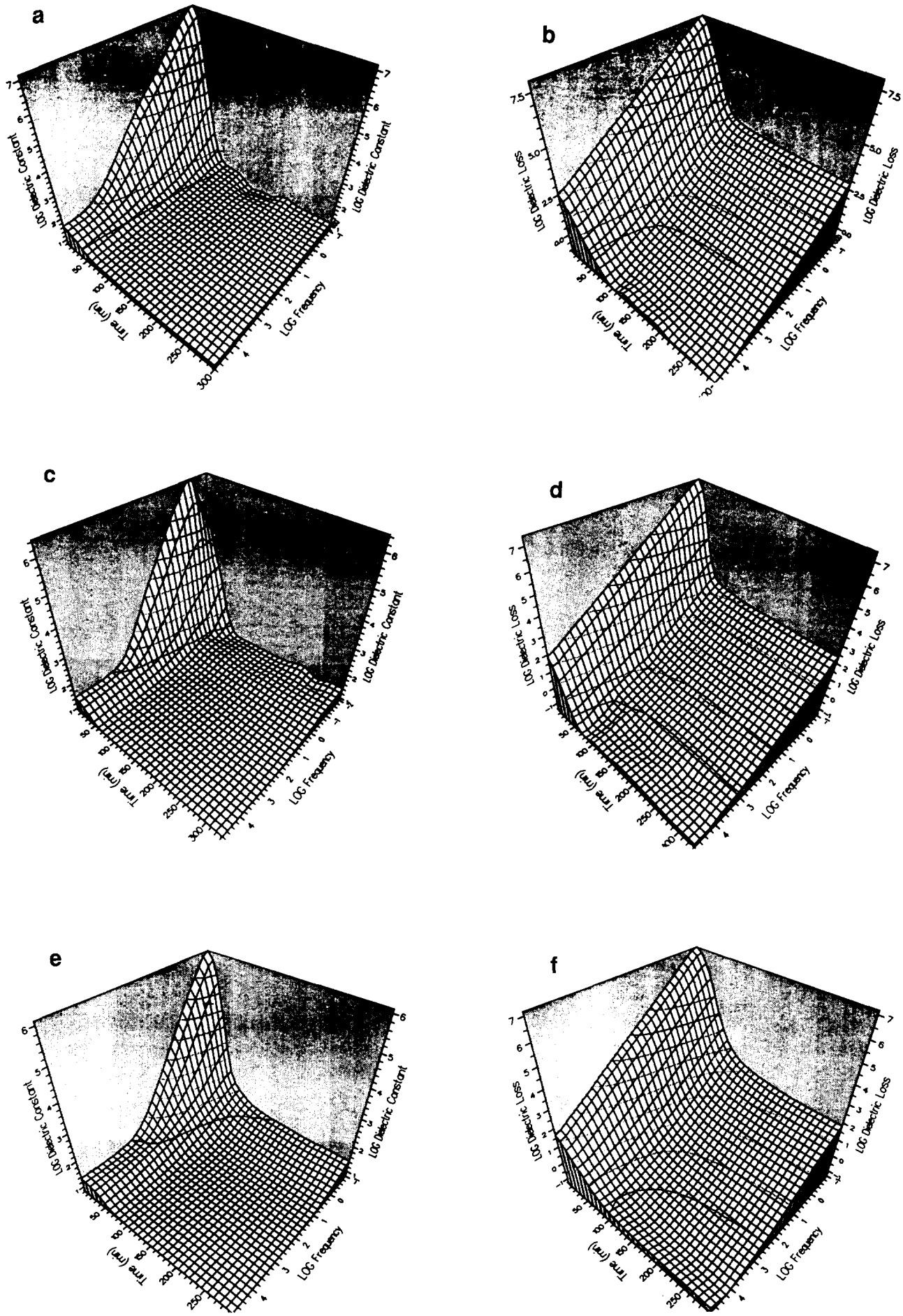

Figure 4 Dielectric constant and loss measured as a function of frequency and time. (a), (b) Cure of MY0510/4,4'-DDS at 180°C. (c), (d) Cure of MY0510/4,4'-DDS/26.7% RT-PS(A) at 180°C. (e), (f) Cure of MY0510/4,4'-DDS/39.1% RT-PS(A) at 180°C

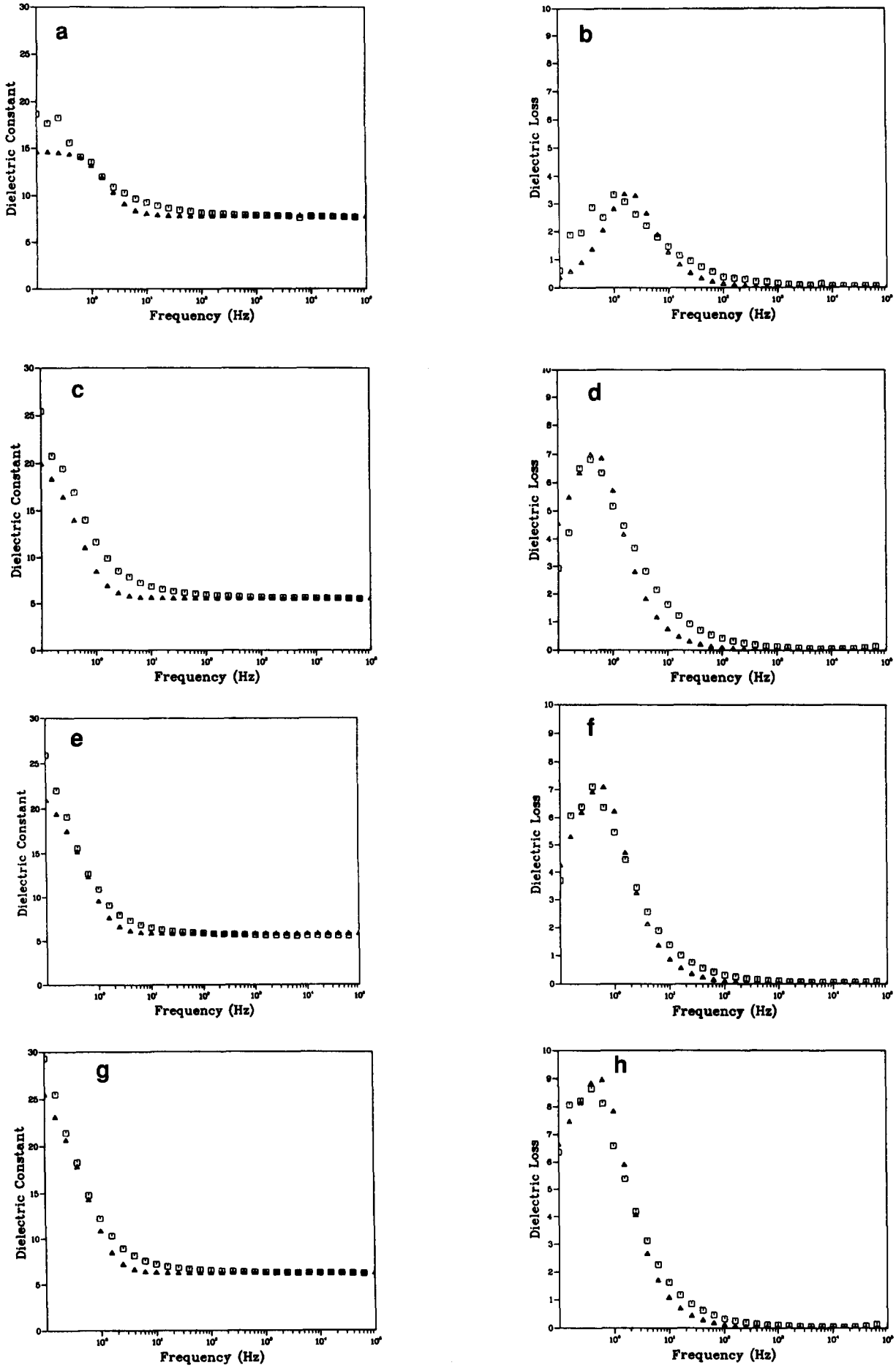

Figure 5 (□) Experimental and (▲) theoretical plots of dielectric constant and loss for cured MY0510/4,4′-DDS/RT-PS(A) measured at 180°C: (a), (b) MY0510/4,4′-DDS/26.7% RT-PS(A); (c), (d) MY0510/4,4′-DDS/30.0% RT-PS(A); (e), (f) MY0510/4,4′-DDS/34.6% RT-PS(A); (g), (h) MY0510/4,4′-DDS/39.1% RT-PS(A)

Table 4 Residual d.c. conductivities of epoxy/thermoplastic blends at 180°C

Thermoplastic (wt%)	D.c. conductivity ($\Omega^{-1}\,m^{-1}$)($\times 10^{-9}$)	
	RT-PS(A)	RT-PS(B)
0.0	4.7	4.7
5.4	0.823	1.86
11.0	0.144	0.372
15.6	2.52	2.66
20.6	0.112	1.13
26.7	1.78	1.71
30.0	0.437	1.05
34.6	0.247	0.551
39.1	0.229	0.466

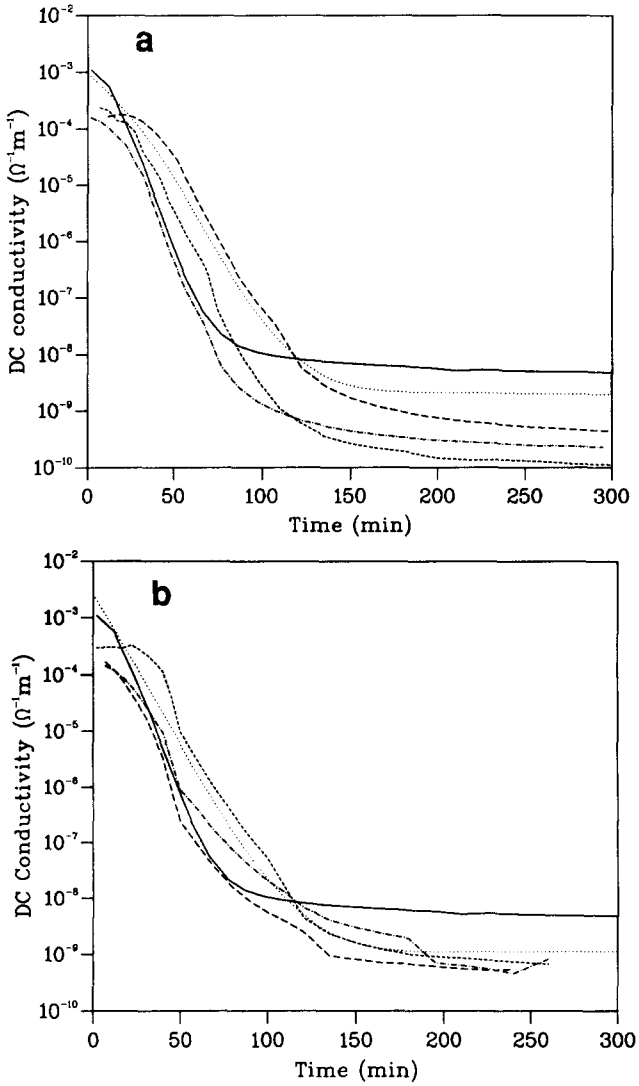

Figure 6 D.c. conductivity monitored during the curing process: (a) MY0510/4,4'-DDS/RT-PS(A) blends at 180°C: ——, 0.0% RT-PS(A); ·····, 11.0% RT-PS(A); -----, 20.5% RT-PS(A); – – –, 30.0% RT-PS(A); –·–·–, 39.1% RT-PS(A). (b) MY0510/4,4'-DDS/RT-PS(B) blends at 180°C: ——, 0.0% RT-PS(B); ·····, 11.0% RT-PS(B); -----, 20.0% RT-PS(B); – – –, 30.0% RT-PS(B); –·–·–, 39.1% RT-PS(B)

asymptotic value. This intercept is not always well defined which may cause discrepancies in the overall trends.

2. A major factor in controlling conductivity in organic materials is the concentration of charge carriers, and so the presence of impurities in the starting materials may give rise to differences in conductivity.
3. Other minor errors may include: differences in the sample thickness leading to varying rates of cure, and possibly differences in the time for the sample to reach a steady temperature. Strenuous efforts were made to minimize these sources of error.

However, the vitrification data do show some consistencies in that the values obtained from ε', ε'' and σ' at any particular level of thermoplastic are in reasonable agreement with each other. The vitrification point at which cessation of dipolar reorientation occurs, can be ascertained by plotting the dielectric constant and loss as a function of time at a frequency of 10 kHz (*Figures 7a* and *b*). The point at which the dielectric constant and loss reach an asymptotic value can be used as a measure of the vitrification point for these materials, and the results of this analysis are also presented in *Table 1*. The inclusion of thermoplastic into the matrix leads to an inhibition of the vitrification point as shown in *Table 3*. The level of the residual d.c. conductivity also varies with the level of thermoplastic (*Table 4*). A gradual reduction in the conductivity is consistent with the changes in morphology increasing the percolation path for the charges, and also generating trapping sites within the

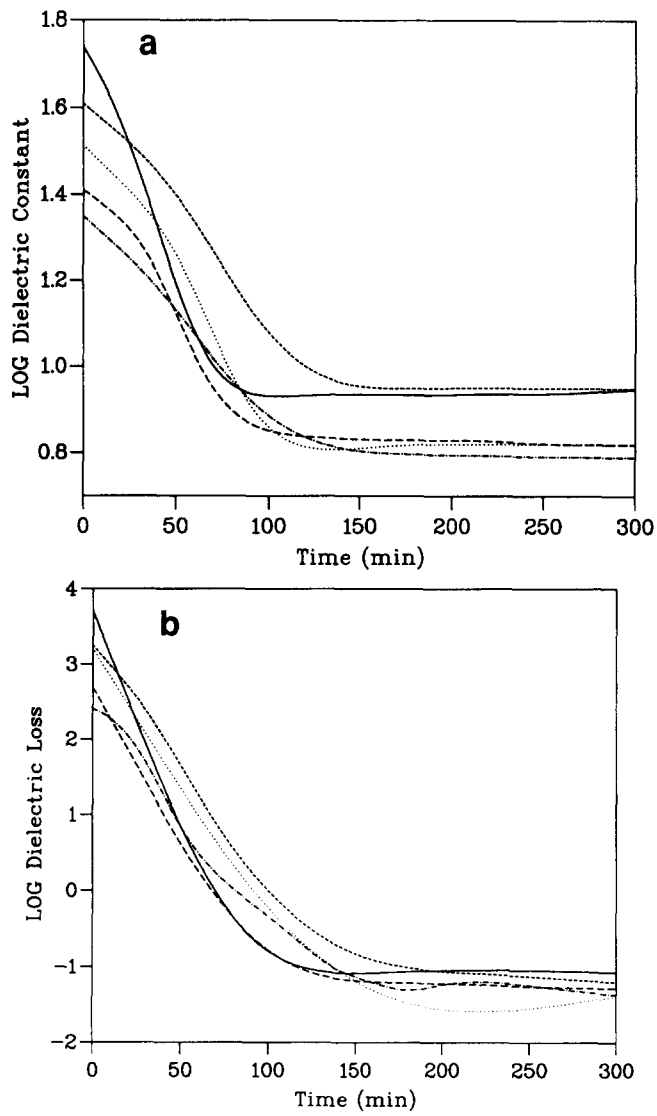

Figure 7 (a) Dielectric constant and (b) dielectric loss monitored at 10 kHz during the cure of MY0510/4,4'-DDS/RT-PS(B) at 180°C: ——, 0.0% RT-PS(B); ·····, 11.0% RT-PS(B); -----, 20.0% RT-PS(B); – – –, 30.0% RT-PS(B); –·–·–, 39.1% RT-PS(B)

Table 5 MWS fitting parameters and dielectric properties for cured MY0510/4,4′-DDS/RT-PS(A) and MY0510/4,4′-DDS/RT-PS(B) blends at 180°C

MY0510/4,4′-DDS/RT-PS(A) blends						MY0510/4,4′-DDS/RT-PS(B) blends		
RT-PS(A) (wt%)	ε'	$\Delta\varepsilon$	σ (Ω^{-1} m^{-1})	V_f	a/b	RT-PS(B) (wt%)	ε'	$\Delta\varepsilon$
26.7	7.8	17.8	2.4×10^{-10}	0.75	0.1	26.7	4.6	2.1
30.0	5.5	20.0	1.5×10^{-10}	0.63	1.2	30.0	6.6	3.4
				0.05	5.0			
34.6	5.8	20.3	2.0×10^{-10}	0.55	1.3	34.6	6.7	5.7
				0.05	5.0			
39.1	6.2	23.1	2.5×10^{-10}	0.55	1.55	39.1	6.1	3.9
				0.05	6.90			

matrix. The scatter in the data is too large for further detailed interpretation.

The gelation times are substantially lower than the corresponding vitrification times owing to the fact that gelation represents the commencement of the three-dimensional network, whereas vitrification represents the completion of the cure.

Dielectric analysis of the cured material

The dielectric spectrum of the fully cured material contains two features; first, a contribution to the loss associated with d.c. conductivity and, second, a loss process only observed in the higher thermoplastic content materials. This latter process we attribute to the MWS effect. An SEM examination of these materials indicates a systematic variation of the morphology with thermoplastic content. At low thermoplastic contents a particulate morphology is observed, the occluded phase being thermoplastic-rich. Correlation of the morphology obtained from the SEM study with the variation in the dielectric properties, indicates that the MWS feature can be associated with the occurrence of the phase-inverted morphology. This would be consistent with the MWS model, which requires the occluded phase to have a higher conductivity than the surrounding matrix, and for a significant magnitude to be observed this phase should approximate to an oblate spheroid.

In order to separate the MWS feature from the conductivity it is necessary to subtract from the loss a contribution which varies according to $1/\omega$. *Figures 5a–h* illustrate the application of the subtraction process; the resultant dielectric loss curve is significantly broader than would be predicted by the simple Debye process, indicating a distribution of relaxation processes. This observation is consistent with the possible distribution in the morphological structure of the material. It can be seen that the position and amplitude of this process vary significantly with thermoplastic content, as would be consistent with the electron micrographs. Using the data from the SEM, theoretical predictions of the MWS process are shown in *Figures 5a–h*. The input data for the theoretical calculations are summarized in *Table 5*. The MWS modelling of the dielectric data from the MY0510/4,4′-DDS/5003P[37] and the MY0510/4,4′-DDS/RT-PS(A), showed good fits which were obtained relatively easily. The magnitude of the dielectric increment was in the region of 35–45. The morphology adopted and the phase size of the inclusions have a profound effect on the magnitude of the relaxation, and the values of the MWS fitting parameters obtained. No suitable fitting could be obtained for the series of materials, MY0510/4,4′-DDS/RT-PS(B) as the magnitude of the relaxation was very small again due to the smaller morphological scale size. The dielectric increment was of the order of ~5, and at low frequency particularly (<1 Hz), this resulted in noise which made the fitting process difficult. The subtraction of the d.c. conductivity contribution from the dielectric loss did not produce a distinct peak, as was the case with each of the previous two series. The results for these blends, 5003P and RT-PS(A) based, show that the dielectric increment varies with composition. For the 5003P system the dielectric increment shows a sharp increase at 20.0 wt% thermoplastic from 4.6 to 57.3, and decreases gradually thereafter with increasing thermoplastic content. In the case of the RT-PS(A) blend the dielectric increment values are smaller, and do not extend to such a large range. The variation in the magnitude of the dielectric relaxations is brought about principally by the differences in the molecular weights of the thermoplastics, which cause varying phase sizes to be formed, and possibly to a lesser extent by differences in the functionality of the end groups. It is clear from the electron micrographs that at all levels of thermoplastic, the RT-PS(A) produces the smaller morphological scale size. In turn, this influences the dielectric properties, specifically the MWS process. The present understanding and model of the MWS theory do not account for the phase size, only the volume fraction, shape and dielectric properties of the constituent phases. The statement therefore that the magnitude of the relaxation is dependent on phase size, is based purely on the experimental observations. The values of the d.c. conductivity of the inclusions required to produce a good fit are consistently larger for the 5003P system, and this is probably reflected by the difference in phase sizes. This is also the case with the shape factor, a/b. The appearance of the MWS feature is observed at thermoplastic levels of 20.6% and above.

The main variables in the MWS theory are the volume fraction of the occluded conducting phase, the dielectric constant of the matrix, and the shape of the occluded phase (defined in terms of the length a to breadth b projected in the field direction). The dielectric constant of the matrix is, however, not a variable as it is measured experimentally as the asymptotic level of the frequency plots, and a value at ~1 kHz was used in the theoretical calculations. The shape of the loss curve figures is very sensitive to the subtraction of the d.c. conductivity; too

large a value artificially sharpens the peak (by reducing the amplitude at low frequency), whereas too small a value leads to the reverse effect. The conductivity of the occluded phase is determined by adjusting the theoretical prediction to give a good fit of the high frequency side of the MWS peak. A single component was fed into the theory for the first comparison with the experimental data. The volume fraction was shown to be that obtained from chemical analysis, and the a/b ratio was adjusted to fit the observed amplitude. In practice it was found that adjustment of the conductivity value was also necessary to obtain agreement between experiment and theory for the high frequency side of the loss, and that this value was lower than that for the pure conducting phase. Having fixed the conductivity, the volume fraction of the occlusion was adjusted to give a better fit of the dielectric loss.

In practice the a/b ratio is quite small, and having this value produces a situation where it is not possible to fit both the dielectric constant and dielectric loss. In every case there is a significant low frequency contribution to the dielectric constant, and this is modelled by the addition of a second component of high a/b ratio. Morphologically this is the same as the occurrence of a very small amount of the co-continuous phase in the matrix. The a/b ratio should ideally tend to unity for a morphology of conducting spheres in a non-conducting matrix and the occurrence of a small fraction of structures with a higher value may be attributed to the presence of fused elongated structures similar to those existing in the co-continuous phase region. For the data fitting process the choice of d.c. conductivity is sensitive to the morphology and is not, therefore, unique.

The feature observed is thus quite clearly interfacial polarization or the MWS process, and illustrates the potential of the dielectric technique to sense morphology. Better fits could be obtained by slightly altering the value of σ, and by the addition of more elements (v and a/b). However, due to the uncertainty in the d.c. conductivity subtraction process mentioned above, this does not always reflect the true situation.

CONCLUSIONS

The dielectric method is capable of providing a detailed understanding, at a molecular level, of the suppression of molecular mobility associated with the gelation and vitrification processes. This paper indicates the value of the dielectric method in the characterization of the morphology of a heterogeneous thermoset system during the course of the cure process. Further studies on this topic will be presented in a subsequent paper.

ACKNOWLEDGEMENT

One of us (AJM) wishes to thank the SERC and ICI plc for support in the form of a co-operative research grant, for the period during which this study was undertaken.

REFERENCES

1 Hayward, D., Mahoubian-Jones, M. G. B. and Pethrick, R. A. *J. Phys. E* 1984, **17**, 683
2 Senturia, S. D. and Sheppard Jr, N. F. *Adv. Polym. Sci.* 1986, **80**, 1
3 Kranbuehl, D., Delos, S., Hoff, M., Haverty, P., Freeman, W., Hoffman, R. and Godfrey, J. *Polym. Eng. Sci.* 1989, **29**, 285
4 Kranbuehl, D., Haverty, P. and Hoff, M. *Polym. Eng. Sci.* 1989, **29**, 988
5 Lee, H. and Neville, K. 'Handbook of Epoxy Resins', McGraw-Hill Co., New York, 1967
6 Potter, W. G. 'Epoxide Resins', Springer, New York, 1970
7 May, C. A. and Tanaka, G. Y. (Eds) 'Epoxy Resin Chemistry and Technology', Marcel Dekker, New York, 1973
8 Bucknall, C. B. 'Toughened Plastics', Wiley, New York, 1977
9 Bucknall, C. B. and Partridge, I. K. *Polym. Eng. Sci.* 1986, **26**, 54
10 Bucknall, C. B. and Partridge, I. K. *Polymer* 1983, **24**, 639
11 Bucknall, C. B. and Gilbert, A. H. *Polymer* 1989, **30**, 213
12 Cecere, J. A., Senger, J. S. and McGrath, J. M. *32nd Int. SAMPE Symp.* 1987, 1276
13 Hedrick, J. L., Yilgor, I., Jurek, M., Hedrick, J. C., Wilkes, G. L. and McGrath, J. E. *Polymer* 1991, **32**, 2020
14 Sefton, M. S., McGrail, P. T., Peacock, J. A., Wilkinson, S. P., Crick, R. A., Davies, M. and Almen, G. *19th Int. SAMPE Tech. Conf.* 1987, 700
15 Shimp, D. A., Hudock, F. A. and Bobo, W. S. *18th Int. SAMPE Tech. Conf.* 1986, 851
16 Stenzenberger, H. D., Romer, W., Herzag, M. and Konig, P. *33rd Int. SAMPE Symp.* 1988, 1546
17 Sefton, M. S., McGrail, P. T., Eustace, P., Chisholm, M., Carter, J. T., Almen, G., MacKenzie, P. D. and Choate, M. *3rd Int. Conf. on Crosslinked Polymers* 1989, 700
18 Iijima, T., Tomoi, M., Tochimoto, T. and Kakiuchi, H. *J. Appl. Polym. Sci.* 1991, **43**, 463
19 Yamanaka, K. and Inoue, T. *Polymer* 1989, **30**, 662
20 Ohnaga, T., Maruta, J. and Inoue, T. *Polymer* 1989, **30**, 1845
21 May, C. *Am. Chem. Soc. Symp. Ser.* 1983, **227**
22 Dawkins, J. 'Developments in Polymer Characterization', Applied Science, Englewood, 1982
23 Hayward, D., Trottier, E., Collins, A., Affrossman, S. and Pethrick, R. A. *J. Oil Col. Chem. Assoc.* 1989, 452
24 Barlow, A. J., Erginsav, A. and Lamb, J. *Proc. R. Soc. A* 1969, **309**, 473
25 Cochrane, J. and Harrison, G. *J. Phys. E* 1972, **5**, 47
26 Davies, M. and Moore, D. R. *Comp. Sci. Technol.* 1991, **40**, 131
27 Meakins, R. J. *Progr. Dielect.* 1961, **3**, 151
28 Van Beek, L. K. H. *Progr. Dielect.* 1967, **7**, 69
29 Hanai, T. in 'Emulsion Science' (Ed. P. Sherman), Academic Press, London, 1968
30 Baird, M. E. 'Electrical Properties of Polymeric Materials', The Plastics Institute, London, 1973
31 Hedvig, P. 'Dielectric Spectroscopy of Polymers', Adam Hilger, Bristol, 1977
32 North, A. M., Pethrick, R. A. and Wilson, A. D. *Polymer* 1978, **19**, 913
33 North, A. M., Pethrick, R. A. and Wilson, A. D. *Polymer* 1978, **19**, 923
34 Siriwittayakorn, T. *PhD Thesis* University of Strathclyde, 1991
35 McCrum, N., Read, B. and Williams, G. 'Anelastic and Dielectric Effects in Polymer Solids', John Wiley and Sons, London, 1967
36 Hill, N. E., Vaughan, W. E., Price, A. H. and Davis, M. 'Dielectric Properties and Molecular Behaviour', van Nostrand Reinhold Company, New York, 1969
37 Mackinnon, A. J., Jenkins, S. D., McGrail, P. T. and Pethrick, R. A. *Macromolecules* 1992, **25**, 3492
38 Huang, Y., Kinloch, A. J and Yuen, M. L. 'Third European Symposium on Polymer Blends', Plastics and Rubber Institute, London, 1990, E5/1
39 Oshima, J. and Sasaki, I. *Polym. News* 1991, **16**, 198
40 Donald, A. M. and Kramer, E. J. *J. Mater. Sci.* 1982, **17**, 1765
41 Bucknall, C. B. *Makromol. Chem., Makromol. Symp.* 1988, **16**, 207
42 Borggreve, R. J. M. and Gaymans, R. J. *Polymer* 1989, **30**, 71
43 Hedrick, J. L., Yilgor, I., Jurek, M., Hedrick, J. C., Wilkes, G. L. and McGrath, J. E. *Polymer* 1991, **32**, 2020
44 MacDonald, J. R. *Phys. Rev.* 1953, **92**, 4
45 MacDonald, J. R. *J. Electrochem. Soc.* 1988, **135**, 2274
46 Bidstrup, W. W., Sheppard, N. F. and Senturia, S. D. *Polym. Sci. Eng.* 1986, **26**, 358